

Published in final edited form as:

*J Magn Reson Imaging*. 2011 November ; 34(5): 1143–1150. doi:10.1002/jmri.22733.

## Measurement of Human Skeletal Muscle Oxidative Capacity by <sup>31</sup>P-MRS: A Cross-Validation with *in vitro* measurements

Ian R. Lanza, PhD<sup>1</sup>, Sumit Bhagra, MD<sup>1</sup>, K. Sreekumaran Nair, MD, PhD<sup>1</sup>, and John D. Port, MD, PhD<sup>2</sup>

<sup>1</sup>Division of Endocrinology, Mayo Clinic College of Medicine, 200 First St SW, Rochester, MN 55905

<sup>2</sup>Division of Radiology, Mayo Clinic College of Medicine, 200 First St SW, Rochester, MN 55905

### Abstract

**Purpose**—To cross-validate skeletal muscle oxidative capacity measured by <sup>31</sup>P-MRS with *in vitro* measurements of oxidative capacity in mitochondria isolated from muscle biopsies of the same muscle group in 18 healthy adults.

**Materials and Methods**—Oxidative capacity *in vivo* was determined from PCr recovery kinetics following a 30s maximal isometric knee extension. State 3 respiration was measured in isolated mitochondria using high-resolution respirometry. A second cohort of 10 individuals underwent two <sup>31</sup>P-MRS testing sessions to assess the test-retest reproducibility of the method.

**Results**—Overall, the *in vivo* and *in vitro* methods were well-correlated ( $r = 0.66 - 0.72$ ) and showed good agreement by Bland Altman plots. Excellent reproducibility was observed for the PCr recovery rate constant (CV = 4.6%, ICC = 0.85) and calculated oxidative capacity (CV = 3.4%, ICC = 0.83).

**Conclusion**—These results indicate that <sup>31</sup>P-MRS corresponds well with gold-standard *in vitro* measurements and is highly reproducible.

### Keywords

phosphocreatine recovery; skeletal muscle; high-resolution respirometry; mitochondria; oxidative capacity

---

Mitochondria are widely recognized for their ability to generate chemical energy to fuel cellular energy requirements. In metabolically active tissues such as skeletal muscle, the abundance and function of these organelles correlates with physical performance (1). More recently there has been growing interest in understanding how these organelles are involved in the etiology or pathophysiology of many human diseases such as type 2 diabetes (2), obesity (3), heart failure (4), stroke (5), and Alzheimer's Disease (6). Historically, mitochondrial function in human skeletal muscle has been estimated from activities of marker enzymes (7) or from direct measurements of oxygen consumption (8) or ATP production rates (9) in tissues or isolated mitochondria. Muscle biopsy specimens also permit measurements of mRNA, DNA, and protein expression measurements. In spite of the wealth of information afforded by *in vitro* measurements from biopsy tissue, practical and ethical considerations limit the frequency and location of tissue biopsies as well as subject populations such as children or frail elderly. Since Chance and colleagues pioneered the use

of phosphorous magnetic resonance spectroscopy ( $^{31}\text{P}$ -MRS) for *in vivo* assessment of human skeletal muscle metabolism (10), this non-invasive technology has become widespread. The capability for non-invasive assessment of skeletal muscle oxidative capacity holds appeal for investigators who desire an *in vivo* measurement that can be performed repeatedly with minimal risk to participants.

Skeletal muscle oxidative capacity may be measured *in vivo* using  $^{31}\text{P}$ -MRS by monitoring the recovery of phosphocreatine (PCr) following prior depletion by a stimulus such as exercise. Through the equilibrium of the creatine kinase reaction, post-exercise PCr resynthesis is a function of mitochondrial ATP production. Thus, the rate constant of PCr recovery ( $k_{\text{PCr}}$ ) is proportional to muscle mitochondrial oxidative capacity, calculated as the product of  $k_{\text{PCr}}$  and PCr concentration in resting skeletal muscle (11–13). This kinetic analysis has been found to be reproducible (14–16) and well-correlated with citrate synthase activity measured *in vitro* (17,18), whole body oxygen uptake (16–20), and theoretical models (17,21). In spite of good agreement between  $^{31}\text{P}$ -MRS and mitochondrial enzyme activity, to our knowledge there have been no comparisons of skeletal muscle oxidative capacity measured by  $^{31}\text{P}$ -MRS and more direct *in vitro* measurements of mitochondrial oxidative capacity. An evaluation of the level of agreement between  $^{31}\text{P}$ -MRS and gold-standard *in vitro* measurements of skeletal muscle oxidative capacity would help establish  $^{31}\text{P}$ -MRS as a valuable tool in research and clinical settings. In the present study we cross-validated skeletal muscle oxidative capacity measured by  $^{31}\text{P}$ -MRS and by high-resolution respirometry of mitochondria isolated from muscle biopsy tissue. We also assessed the test-retest reliability of oxidative capacity measured by  $^{31}\text{P}$ -MRS.

## MATERIALS and METHODS

### Subjects

Eighteen healthy participants (11 male, 7 female) (mean age  $\pm$  SD =  $38 \pm 10$  yrs, mass =  $73.5 \pm 9.6$  kg, height =  $170 \pm 10$  cm) were included in the study after providing written informed consent, as approved by the Mayo Clinic Institutional Review Board. Potential participants were excluded if any history of metabolic or cardiovascular disease, plasma glucose  $>99$  mg/dl, BMI  $>28$  kg/m<sup>2</sup>, medications affecting outcome measures, anemia, pregnancy, and substance abuse. Participants consumed a weight-maintaining diet for 3 days before the study. On the evening of day 3 of the diet, participants were admitted to the Mayo Clinic CTSA Clinical Research Unit, given a standardized meal and snack at 1800h and 2200h.

### Mitochondrial Oxidative Capacity Measured *in vitro*

The following morning, a percutaneous needle muscle biopsy was obtained from the vastus lateral is muscle of the left leg under local anesthesia (2% lidocaine). Mitochondria were isolated from fresh, non-frozen muscle tissue using methods described previously (22). Briefly, muscle was transferred into a chilled glass dish containing an ionic homogenizing buffer (100 mM KCl, 50 mM Tris, 5 mM MgCl<sub>2</sub>, 1.8mM ATP, and 1mM EDTA, pH 7.2). Tissue was minced, incubated on ice for 2 minutes with protease, rinsed, and gently homogenized on ice for 10 minutes using a motor-driven Potter-Elvehjem tissue grinder. Mitochondria were separated by differential centrifugation and resuspended in a nonionic buffer (225 mM sucrose, 44 mM KH<sub>2</sub>PO<sub>4</sub>, 12.5 mM Mg acetate, and 6 mM EDTA).

Respiration of isolated mitochondria was performed using the Oxygraph-2k (Oroboros Instruments, Innsbruck, Austria) with continuous stirring and temperature maintained at 37°C. Experiments were performed in respiration buffer (MiRO5) containing 110 mM sucrose, 60 mM potassium lactobionate, 0.5 mM EGTA, 1 g/L BSA essentially fat free, 3

mM MgCl<sub>2</sub>, 20 mM taurine, 10 mM KH<sub>2</sub>PO<sub>4</sub>, 20 mM Hepes, pH 7.1. Mitochondria were allowed to equilibrate in MiRO5 until stable oxygen flux rates were achieved. After equilibration, a stepwise titration protocol was initiated, starting with the addition of glutamate (10mM) and malate (2mM) in the absence of exogenous adenylates to initiate state 2 respiration with electron flow through complex I. State 3 respiration was initiated by the addition of ADP (2.5mM). The addition of succinate (10mM) provided convergent electron flow through respiratory chain complexes I and II, followed by rotenone (0.5 μM) to inhibit complex I. State 4 respiration was measured in the presence of oligomycin (2μg/ml) to inhibit ATP synthase. Oxygen flux rates were calculated and corrected for background oxygen kinetics using Datlab software (Oroboros Instruments, Innsbruck, Austria) and expressed per tissue wet weight. Respiratory control ratios (RCR) were calculated as the quotient of state 3 and state 4 fluxes. The mean RCR value of 8.5±0.75 indicates high-quality mitochondrial preparation. As an additional quality control measure, we added 10μM cytochrome c during state 3 respiration to test the intactness of the outer mitochondrial membrane. Exogenous cytochrome c resulted in less than 5% increase in respiration rates (data not shown), indicating that the organelles were largely intact.

### Oxidative Capacity Measured by Magnetic Resonance Spectroscopy *in vivo*

Following the muscle biopsy, participants continued the weight-maintaining diet for the rest of the day, stayed overnight in the clinical research unit, and remained fasting from 2200h until the completion of the <sup>31</sup>P-MRS studies the following morning. At 0800h on day 2, participants were transported by wheelchair to the Mayo Clinic Center for Advanced Imaging Research for *in vivo* measurement of muscle oxidative capacity. The test-retest reliability of muscle oxidative capacity measured by <sup>31</sup>P-MRS was determined in 10 participants who repeated the *in vivo* metabolic testing within 10 days of the initial test. Although our comparison of *in vitro* to *in vivo* measurements took place in the carefully controlled environment of an inpatient clinical research unit where food intake and physical activity were tightly regulated for several days before the measurements, we wanted to assess the reproducibility of <sup>31</sup>P-MRS under the more typical conditions of a clinical outpatient setting. Therefore reproducibility was measured in a separate cohort of individuals who were asked to report to the MR research center at 8:00am after abstaining from food, alcohol, or caffeine from 2200h the previous evening and avoiding strenuous exercise for 24 hours. The coil was positioned over the muscle in the same manner for both tests using anatomical landmarks. Participants were positioned supine on the patient bed of a 3.0 Tesla GE Signa MRI scanner. The right leg was positioned in a custom-made exercise apparatus designed to measure isometric knee extension force. Force data was digitized at 10hz and the calibrated signal was integrated to determine the total “work”, defined as the force-time integral. Visual force feedback was provided to participants on a computer display. Participants were briefly habituated to the task of maximal isometric knee extension. With visual force feedback and verbal encouraging from the investigators, volunteers performed 3–4 brief (5–10s) “practice” efforts until subsequent trials differed by no more than 10% by visual inspection of the computer display. Thereafter, the computer display was calibrated to each participant’s maximal effort to ensure that they were able to reach the same force output during the actual exercise protocol. A 5-inch diameter circular transmit/receive phosphorous radiofrequency coil was placed over the vastus lateralis muscle and held in place with an elastized wrap. Gradient-echo scout images and T1-weighted axial images along the femur were used to confirm proper positioning of the leg in the isocenter of the magnet, and proper positioning of the phosphorus coil over the vastus lateralis muscle. Following proton image acquisition, the magnet was manually shimmed on the muscle phosphorous signal yielding a full width at half-maximal height of the unfiltered PCr peak of 12.1 ± 2.4 Hz (mean ± SD). Two phosphorus acquisitions in resting muscle were obtained (transmit power tuned to 90 degree flip angle, 500 ms RF pulse, spectral

width=2500 Hz, data points=2048), one fully relaxed spectrum (TR=16s) and one partially saturated spectrum using a short repetition time (TR=2s). Correction factors for partial saturation at the 2s TR were determined for each participant for inorganic phosphate (Pi), phosphocreatine (PCr), and ATP. Next, a single phosphorus acquisition in exercising muscle was obtained (TR=2s), starting with 60s of rest, 30s of maximal effort sustained isometric knee extension, and 10 minutes of recovery. Free induction decays were averaged to yield temporal resolution of 1 minute at rest, 2s during exercise and, 6s during the first 5 minutes of recovery, and 10s during the final 5 minutes of recovery. A stacked plot of rest, exercise, and recovery spectra for a typical participant is shown in Figure 1.

### Spectral Analysis and Metabolic Calculations

Free induction decays were processed first by exponential multiplication corresponding to 5 Hz line broadening, followed by conversion to the frequency domain by Fourier transform. Spectra were manually phased, and the underlying broad peak due to the phosphorous in bone was removed by calculating a 5th order polynomial fit of the baseline region. The areas of peaks corresponding to PCr, Pi, and  $\gamma$  ATP were measured by curve-fitting software (NUTS software, Acorn NMR, Livermore, CA, USA). Millimolar concentrations of phosphorous metabolites were calculated assuming that  $[PCr] + [Cr] = 42.5$  mM and resting  $[ATP] = 8.2$  mM (23). An assumption that  $\Delta[Pi]$  is equivalent to  $\Delta[Cr]$  during rest, exercise, and recovery is based on the equilibrium of the creatine kinase reaction and impermeability of the muscle cells to Pi and free creatine (24). Intramuscular pH was calculated based on the chemical shift ( $\sigma$ ) of Pi relative to PCr in parts per million:

$$pH = 6.75 + \log \frac{\sigma - 3.27}{5.69 - \sigma}$$

Skeletal muscle oxidative capacity ( $Q_{max}$ ) was determined from the kinetics of PCr recovery after the 30s muscle contraction. For each participant, a rate constant ( $k_{PCr}$ ) of PCr recovery was determined by fitting a single exponential curve:

$$PCr(t) = \Delta PCr(1 - e^{-k_{PCr}t}) + PCr_{ex}$$

Where  $t$  is time,  $PCr_{ex}$  is  $[PCr]$  at the end of exercise,  $\Delta PCr = (PCr_{rest} - PCr_{ex})$ . Previous studies have established that the rate constant of PCr recovery reflects the rate of oxidative phosphorylation (13). Vastus lateralis oxidative capacity ( $Q_{max}$ , mM ATP/s) was determined as the product of  $k_{PCr}$  and  $PCr_{rest}$  (11,12,25).

### Statistical Analyses

Data are presented as mean  $\pm$  SEM unless otherwise indicated. The association between muscle oxidative capacity measured by  $^{31}P$ -MRS and high-resolution respirometry was determined from Pearson's correlation coefficients. The level of agreement between  $^{31}P$ -MRS and high-resolution respirometry was determined by Bland-Altman plots using computed Z scores for each measurement. Test-retest reliability was determined using coefficient of variation as an index of absolute reliability and intraclass correlation coefficients as an index of relative reliability (26). Paired t-tests were used to test for possible statistical differences between testing sessions in variables measured during the reliability studies. Statistical analyses were performed using SAS and JMP software (Cary, NC).

## RESULTS

### High-resolution respirometry in isolated mitochondria

We expressed oxygen flux rates per tissue weight to provide an *in vitro* index of mitochondrial capacity that is sensitive to both intrinsic organelle function as well as the abundance of mitochondria in the muscle tissue. Alternatively, the influence of tissue mitochondrial content is often removed by normalizing oxygen flux rates to mitochondrial protein content, citrate synthase activity, or mitochondrial DNA copy number. This approach provides an index of intrinsic mitochondrial function that is independent of mitochondrial content. We chose to express the data per tissue weight rather than normalizing to mitochondrial content because it better represents the *in vivo* situation where oxidative capacity is a function of both intrinsic function and mitochondrial abundance. Respiring mitochondria isolated from muscle biopsy tissue demonstrated the expected patterns in response to the stepwise substrate-inhibitor titration protocol (Table 1). Specifically, in the presence of complex I substrates (glutamate + malate) without exogenous adenylates (State 2), mitochondrial respiration was minimal ( $36.1 \pm 2.8$  pmol/s/mg). Addition of 2.5 mM ADP to stimulate state 3 resulted in a nearly 20-fold increase in oxygen consumption ( $698.7 \pm 64.2$  pmol/s/mg). When succinate was added to provide convergent electron flow through complexes I and II, oxygen flux nearly doubled ( $1175.6 \pm 91.4$  pmol/s/mg). Inhibiting complex I by rotenone decreased oxygen flux to  $747.5 \pm 54.4$  pmol/s/mg, representing state 3 through complex II exclusively. When oligomycin was added to inhibit ADP phosphorylation (state 4), respiration rates decreased to  $165.2 \pm 28.5$  pmol/s/mg. The respiratory control ratio, calculated as the quotient of state 3 to state 4, was  $8.50 \pm 0.75$ , indicating good coupling and high quality mitochondrial preparation.

### Phosphorous metabolites, pH, and oxidative capacity *in vivo*

The resting values for [PCr], [Pi], and pH were  $38.10 \pm 0.24$  mM,  $4.39 \pm 0.24$  mM, and  $7.03 \pm 0.004$ , respectively (Table 1). These values are in close agreement with previously published values in resting human skeletal muscle (12,13,27). A representative stackplot of phosphorous spectra during rest, exercise, and recovery is shown in Figure 1. During the 30s sustained isometric muscle contraction, PCr decreased by approximately 20% to  $30.73 \pm 0.88$  mM with a reciprocal increase in Pi to  $11.77 \pm 0.88$  mM (Figure 2, Table 1). Intramuscular pH demonstrated an initial alkalosis during exercise, followed by slight acidosis during recovery, consistent with the proton stoichiometry of the creatine kinase reaction (Figure 2, Table 1). Importantly, the exercise bout was designed to decrease [PCr] without inducing acidosis to avoid pH effects on mitochondrial ATP synthesis and the equilibrium of the creatine kinase reaction. End-exercise pH was  $7.07 \pm 0.009$ . The PCr recovery rate constant was  $0.034 \pm 0.002$ , and the computed oxidative capacity was  $1.29 \pm 0.08$  mM ATP/s, values which are in close agreement with previous reports in vastus lateralis muscle of young healthy individuals (25,27).

### Relationship between oxidative capacity measured *in vitro* and *in vivo*

The linear dependence between oxidative capacity measured by  $^{31}\text{P}$ -MRS and high-resolution respirometry was determined from the Pearson correlation coefficient of the two variables (Figure 3). Oxidative capacity measured by  $^{31}\text{P}$ -MRS was well-correlated with state 3 respiration with substrates for complex I ( $r=0.717$ , Figure 3A), substrates for complex I + II ( $r=0.710$ , Figure 3B), and substrates for complex II ( $r=0.664$ , Figure 3C). Bland-Altman plots of the standardized Z-scores (Figure 3D, E, F) shows that the errors (differences between  $Q_{\text{max}}$  and state 3 measurements) were approximately symmetrically distributed vertically around zero, indicating that there was no systematic bias in the *in vivo* measurements compared with *in vitro* measurements.

## Reproducibility of oxidative capacity measured by $^{31}\text{P}$ -MRS

One participant from the reproducibility cohort was excluded for failing to adhere to the study guidelines by engaging in strenuous exercise the morning of the second study. Resting and end-exercise values for [PCr], [Pi], and pH for measurements repeated on two separate testing sessions are given in Table 2. The CVs were less than 3% for resting PCr and pH, but higher (14.6%) for resting Pi. The CVs for end-exercise PCr (10%) and pH (0.6%) were slightly higher than observed at rest. Individual  $k_{\text{PCr}}$  and  $Q_{\text{max}}$  values are displayed in Figure 4. The CV values corresponding to  $k_{\text{PCr}}$  and  $Q_{\text{max}}$  were 4.65 and 3.37%, respectively. The ICC values for  $k_{\text{PCr}}$  and  $Q_{\text{max}}$  were 0.85 and 0.83, respectively. Resting and end-exercise PCr, Pi, and pH were similar between the two testing sessions ( $P > 0.05$  by paired ttest, Table 2), as were  $K_{\text{PCr}}$ ,  $Q_{\text{max}}$ , and FTI (Table 2).

## DISCUSSION

The current study demonstrates for the first time that skeletal muscle oxidative capacity measured by  $^{31}\text{P}$ -MRS *in vivo* correlates moderately well with oxidative capacity measured by high-resolution respirometry in mitochondria isolated from human muscle biopsies with good agreement between the two independent measurements. We also demonstrate excellent test-retest reliability of muscle oxidative capacity measured by  $^{31}\text{P}$ -MRS. Given the widespread use of  $^{31}\text{P}$ -MRS to measure oxidative capacity from PCr recovery kinetics, there is critical need for direct comparisons with gold-standard *in vitro* methods. The good agreement with measurements in isolated mitochondria and high reproducibility of  $^{31}\text{P}$ -MRS supports the growing use of  $^{31}\text{P}$ -MRS as a viable tool for research and clinical investigation of mitochondrial function *in vivo*.

*In vitro* measurements such as maximal enzyme activities, ATP production rates, and oxygen consumption in tissue samples or isolated mitochondria provide essential information to characterize mitochondrial physiology. An acknowledged limitation of these measurements is that they are performed *in vitro* under optimal conditions and may not accurately represent the *in vivo* function of organelle. Furthermore, isolated mitochondria are stripped of important regulatory signals that would otherwise be present in the intact cell (28). This possibility was recently highlighted in a recent report that age-related impairments in mitochondrial function were evident in isolated mitochondria, but not in permeabilized muscle fiber preparations, which more closely approximate true *in vivo* physiology (29). *In vivo* measurement of muscle oxidative capacity by  $^{31}\text{P}$ -MRS overcomes many of these limitations, but is dependent on several critical assumptions (e.g., stable [ATP], negligible glycolysis during recovery, exponential recovery of PCr). These assumptions are supported by sound biochemical theory, but have not all been proven empirically. A direct comparison of *in vitro* and *in vivo* measurements of mitochondrial capacity is essential to evaluate the level of agreement between independent measurements.

Muscle oxidative capacity measured by  $^{31}\text{P}$ -MRS has previously been compared with *in vitro* markers of mitochondrial function. McCully et al. were the first to make this comparison in the lateral gastrocnemius muscles of human volunteers (17). These investigators demonstrated that  $k_{\text{PCr}}$  was well-correlated ( $r=0.71$ ) with citrate synthase activity and whole-body peak  $\text{VO}_2$  (17). Several years later, another group reported a moderate correlation between  $^{31}\text{P}$ -MRS measurements and citrate synthase activity ( $r=0.48$  to  $0.64$ ) in calf muscle (18) as well as whole-body  $\text{VO}_{2\text{ peak}}$  (16). A study in rat gastrocnemius muscle also found a strong correlation ( $r=0.84$ ) between  $k_{\text{PCr}}$  and citrate synthase activity (21). The present study builds on these early observations by examining the relationship between oxidative capacity measured by  $^{31}\text{P}$ -MRS and oxidative capacity measured directly from freshly isolated, intact, functional mitochondria. Rather than measuring the maximal activity of a single enzyme, we measured the maximal rates of

oxygen consumption (state 3) in functional, intact organelles with substrate combinations providing electron flow into respiratory chain complex I, complexes I + II, and complex II. Consistent with earlier comparisons with citrate synthase activity, we found that state 3 respiration was well-correlated with oxidative capacity measured by  $^{31}\text{P}$ -MRS. The correlation between *in vivo* and *in vitro* measurements of oxidative capacity show that similar relative results are generated by both methodologies in spite of the acknowledged limitations of each analytical method mentioned earlier. Future studies are needed to determine if there is good agreement between *in vivo* and *in vitro* measurements in clinical situations such as cardiovascular disease, type 2 diabetes, or aging where mitochondrial function may be impaired. Some insight comes from a study showing good correlation between *in vivo* oxidative capacity measured by  $^{31}\text{P}$ -MRS, succinate dehydrogenase activity, and whole body  $\text{VO}_2$  peak (20).

Direct comparison of absolute values between the two methodologies is problematic for several reasons. First, the *in vitro* method measures the maximal rate of oxygen consumption in mitochondria whereas  $^{31}\text{P}$ -MRS measures the maximal rate of ATP production. Although the dogmatic ratio of ATP produced per oxygen consumed is less than 3, this ratio varies considerably across individuals and with different respiratory chain reducing equivalents. It is also difficult to directly compare absolute rates measured by the different methods because respiration rates are measured in the presence of saturating levels of substrates; conditions that are unlikely *in vivo* where multiple enzyme systems are regulated by actual metabolic perturbations. For these reasons we standardized the values for *in vivo* and *in vitro* measurements by computing Z-scores for each observation. Using the Z-scores, we then generated Bland-Altman plots to examine the level of agreement between the two independent measurements. The symmetric vertical distribution about zero and lack of bias indicates good agreement between oxidative capacity measured by  $^{31}\text{P}$ -MRS and high-resolution respirometry in isolated mitochondria.

In addition to comparing  $^{31}\text{P}$ -MRS with *in vitro* measurements of oxidative capacity, we also evaluated the test-retest reproducibility of oxidative capacity measured by  $^{31}\text{P}$ -MRS. Several research groups have reported acceptable reproducibility of PCr recovery kinetics in human muscle (14–16,30). Under modestly controlled outpatient conditions, we find good reproducibility for both the rate constant of PCr recovery and oxidative capacity. Reproducibility measured by coefficient of variation was 4.65 and 3.37% for kPCr and  $Q_{\text{max}}$ , respectively. These values are lower than literature values of 18.4% (14) 11.5% (30), and 28% (15), but close to the value of 4.6% reported during maximal contraction protocol of the plantarflexors (16) and 6.9% for PCr recovery time constant when intracellular pH remained above 6.9 (30). There are several factors that contribute to the within-subject variability of this measurement, including subtle differences in coil positioning, coil loading, position in the isocenter, shim quality, manual aspects of spectral analysis such as phasing and line fitting, diet, exercise, hydration, stress, and compliance with the in-magnet exercise protocol. We attribute the high reproducibility of our measurement to careful control of coil positioning, standardized analysis procedures, subject compliance with dietary and activity restrictions, and thorough familiarization of the participant with the in-magnet exercise protocol. Furthermore, the consecutive measurements in this study were separated by no more than 7 days whereas other studies separated consecutive measurements by up to 30 days (14) or a year (15) which may add variability due to seasonal factors or gradual changes over time. Resting and end-exercise values for phosphorous metabolites and pH also exhibited low CVs with the exception of inorganic phosphate, which averaged 14.6% at rest and 10% at end-exercise. We attribute the higher within-subject variability of Pi to the low signal-to noise of the peak corresponding to this metabolite, which improves during exercise. We also observed somewhat higher within-subjects variability of exercise performance based on the CV of the force-time-integral (7.81%). Although participants were

habituated to the task prior to the first testing session, the FTI values were somewhat higher on the second testing session, indicating some learning effect. In spite of the somewhat higher variability of exercise performance and Pi quantitation, the PCr recovery rate constant and oxidative capacity were highly reproducible. In fact, one advantage of this technique is that work level is not an important factor in PCr recovery kinetics, provided that the pH change in the muscle is minimal (11,31). Conceivably, these measurements could be performed with a very basic in-magnet ergometer without the technical challenge of simultaneous measurement of force output. Although we also observed high reproducibility of end-exercise PCr and pH, it is worth noting that small variations in end-exercise pH and ADP have minimal impact on PCr recovery kinetics (16).

A muscle biopsy represents a very small sample of a very large, heterogeneous muscle. In contrast, our  $^{31}\text{P}$ -MRS measurements were performed using a surface coil with a non-localized acquisition, resulting in a large sampling volume that may have included tissues other than vastus lateralis. Although we are confident that we biopsied the vastus lateralis muscle, we cannot rule out the possibility that vastus intermedius and rectus femoris could have contributed to some of the  $^{31}\text{P}$ -MRS signal. Localized acquisitions from a defined voxel within the boundaries of the vastus lateralis muscle may improve the muscle specificity of the  $^{31}\text{P}$ -MRS acquisition, but there is little that can be done to address the fact that a small muscle biopsy may not accurately represent the phenotype of the whole muscle, short of taking many biopsies across the muscle bed. Given these limitations, we still find good agreement between the two methodologies for measuring muscle oxidative capacity. The kinetic analysis of PCr recovery assumed a monoexponential recovery curve. Others find that PCr recovery is biphasic following intense muscle activity where pH drops below a threshold value of 6.75 (31). By using a short duration maximal contraction, we were able to sufficiently deplete PCr while maintaining pH levels well-above the critical threshold. We assume that the vast majority of motor units are recruited during the maximal effort, although we did not confirm this with electromyography or specific measurements of central motor drive.

In conclusion, the results of this study indicate that skeletal muscle oxidative capacity measured by  $^{31}\text{P}$ -MRS is highly reproducible and in good agreement with measurements of oxidative capacity using a gold-standard *in vitro* measurement. These data provide essential confirmation that the *in vitro* and *in vivo* methods are detecting similar aspects of mitochondrial function.

## Acknowledgments

**Grant Support:** This work was supported by National Institutes of Health (NIH) Grants RO1DK41973 (K.S.N.), KL2RR024151 (I.R.L.), and UL1-RR-025150 from the National Center for Research Resources.

We are grateful for the skillful technical expertise of Jill Schimke, Katherine Klaus, Dawn Morse, Daniel Jakaitis, Bushra Ali, Deborah Kay Sheldon, Roberta Soderberg, Diane Sauter, Mandie Maroney-Smith, and Melissa Aakre. We are also thankful for the support of the Mayo Clinic Center for Translational Sciences Activities Clinical Research Unit. Lastly, we thank all of the participants for their time and dedication to this work.

## References

1. Holloszy JO. Biochemical adaptations in muscle. Effects of exercise on mitochondrial oxygen uptake and respiratory enzyme activity in skeletal muscle. *J Biol Chem.* 1967; 242(9):2278–2282. [PubMed: 4290225]
2. Kelley DE, He J, Menshikova EV, Ritov VB. Dysfunction of mitochondria in human skeletal muscle in type 2 diabetes. *Diabetes.* 2002; 51(10):2944–2950. [PubMed: 12351431]
3. Simoneau JA, Kelley DE. Altered glycolytic and oxidative capacities of skeletal muscle contribute to insulin resistance in NIDDM. *J Appl Physiol.* 1997; 83(1):166–171. [PubMed: 9216960]



4. Neubauer S. The failing heart--an engine out of fuel. *N Engl J Med.* 2007; 356(11):1140–1151. [PubMed: 17360992]
5. Pulkes T, Sweeney MG, Hanna MG. Increased risk of stroke in patients with the A12308G polymorphism in mitochondria. *Lancet.* 2000; 356(9247):2068–2069. [PubMed: 11145497]
6. Ansari MA, Scheff SW. Oxidative stress in the progression of Alzheimer disease in the frontal cortex. *J Neuropathol Exp Neurol.* 2010; 69(2):155–167. [PubMed: 20084018]
7. Coggan AR, Spina RJ, King DS, Rogers MA, Brown M, Nemeth PM, Holloszy JO. Skeletal muscle adaptations to endurance training in 60-to 70-yr-old men and women. *J Appl Physiol.* 1992; 72(5): 1780–1786. [PubMed: 1601786]
8. Gnaiger E. Capacity of oxidative phosphorylation in human skeletal muscle: new perspectives of mitochondrial physiology. *Int J Biochem Cell Biol.* 2009; 41(10):1837–1845. [PubMed: 19467914]
9. Short KR, Bigelow ML, Kahl J, Singh R, Coenen-Schimke J, Raghavakaimal S, Nair KS. Decline in skeletal muscle mitochondrial function with aging in humans. *Proc Natl Acad Sci U S A.* 2005; 102(15):5618–5623. [PubMed: 15800038]
10. Chance B, Leigh JS Jr, Clark BJ, Maris J, Kent J, Nioka S, Smith D. Control of oxidative metabolism and oxygen delivery in human skeletal muscle: a steady-state analysis of the work/energy cost transfer function. *Proc Natl Acad Sci U S A.* 1985; 82(24):8384–8388. [PubMed: 3866229]
11. Meyer RA. A linear model of muscle respiration explains monoexponential phosphocreatine changes. *Am J Physiol.* 1988; 254(4 Pt 1):C548–553. [PubMed: 3354652]
12. Lanza IR, Befroy DE, Kent-Braun JA. Age-related changes in ATP-producing pathways in human skeletal muscle in vivo. *J Appl Physiol.* 2005; 99(5):1736–1744. [PubMed: 16002769]
13. Kent-Braun JA, Ng AV. Skeletal muscle oxidative capacity in young and older women and men. *J Appl Physiol.* 2000; 89(3):1072–1078. [PubMed: 10956353]
14. McCully KK, Turner TN, Langley J, Zhao Q. The reproducibility of measurements of intramuscular magnesium concentrations and muscle oxidative capacity using 31P MRS. *Dyn Med.* 2009; 8:5. [PubMed: 20003509]
15. Layec G, Bringard A, Le Fur Y, Vilmen C, Micallef JP, Perrey S, Cozzone PJ, Bendahan D. Reproducibility assessment of metabolic variables characterizing muscle energetics in vivo: A 31P-MRS study. *Magn Reson Med.* 2009; 62(4):840–854. [PubMed: 19725136]
16. Larson-Meyer DE, Newcomer BR, Hunter GR, Hetherington HP, Weinsier RL. 31P MRS measurement of mitochondrial function in skeletal muscle: reliability, force-level sensitivity and relation to whole body maximal oxygen uptake. *NMR Biomed.* 2000; 13(1):14–27. [PubMed: 10668050]
17. McCully KK, Fielding RA, Evans WJ, Leigh JS Jr, Posner JD. Relationships between in vivo and in vitro measurements of metabolism in young and old human calf muscles. *J Appl Physiol.* 1993; 75(2):813–819. [PubMed: 8226486]
18. Larson-Meyer DE, Newcomer BR, Hunter GR, Joannisse DR, Weinsier RL, Bamman MM. Relation between in vivo and in vitro measurements of skeletal muscle oxidative metabolism. *Muscle Nerve.* 2001; 24(12):1665–1676. [PubMed: 11745976]
19. Takahashi H, Inaki M, Fujimoto K, Katsuta S, Anno I, Niitsu M, Itai Y. Control of the rate of phosphocreatine resynthesis after exercise in trained and untrained human quadriceps muscles. *Eur J Appl Physiol Occup Physiol.* 1995; 71(5):396–404. [PubMed: 8565970]
20. Praet SF, De Feyter HM, Jonkers RA, Nicolay K, van Pul C, Kuipers H, van Loon LJ, Prompers JJ. 31P MR spectroscopy and in vitro markers of oxidative capacity in type 2 diabetes patients. *MAGMA.* 2006; 19(6):321–331. [PubMed: 17180611]
21. Paganini AT, Foley JM, Meyer RA. Linear dependence of muscle phosphocreatine kinetics on oxidative capacity. *Am J Physiol.* 1997; 272(2 Pt 1):C501–510. [PubMed: 9124293]
22. Lanza IR, Nair KS. Functional assessment of isolated mitochondria in vitro. *Methods Enzymol.* 2009; 457:349–372. [PubMed: 19426878]
23. Harris RC, Hultman E, Nordesjo LO. Glycogen, glycolytic intermediates and high-energy phosphates determined in biopsy samples of musculus quadriceps femoris of man at rest. *Methods and variance of values Scand. J Clin Lab Invest.* 1974; 33(2):109–120.

24. Kemp GJ, Radda GK. Quantitative interpretation of bioenergetic data from <sup>31</sup>P and <sup>1</sup>H magnetic resonance spectroscopic studies of skeletal muscle: an analytical review. *Magn Reson Q.* 1994; 10(1):43–63. [PubMed: 8161485]
25. Conley KE, Jubrias SA, Esselman PC. Oxidative capacity and ageing in human muscle. *J Physiol.* 2000; 526(Pt 1):203–210. [PubMed: 10878112]
26. Shrout PE, Fleiss JL. Intraclass correlations: uses in assessing rater reliability. *Psychol Bull.* 1979; 86(2):420–428. [PubMed: 18839484]
27. Larsen RG, Callahan DM, Foulis SA, Kent-Braun JA. In vivo oxidative capacity varies with muscle and training status in young adults. *J Appl Physiol.* 2009; 107(3):873–879. [PubMed: 19556459]
28. Hutter E, Skovbro M, Lener B, Prats C, Rabol R, Dela F, Jansen-Durr P. Oxidative stress and mitochondrial impairment can be separated from lipofuscin accumulation in aged human skeletal muscle. *Aging Cell.* 2007; 6(2):245–256. [PubMed: 17376148]
29. Picard M, Ritchie D, Wright KJ, Romestaing C, Thomas MM, Rowan SL, Taivassalo T, Hepple RT. Mitochondrial functional impairment with aging is exaggerated in isolated mitochondria compared to permeabilized myofibers. *Aging Cell.* 2010; 9(6):1032–1046. [PubMed: 20849523]
30. van den Broek NM, De Feyter HM, de Graaf L, Nicolay K, Prompers JJ. Intersubject differences in the effect of acidosis on phosphocreatine recovery kinetics in muscle after exercise are due to differences in proton efflux rates. *Am J Physiol Cell Physiol.* 2007; 293(1):C228–237. [PubMed: 17392383]
31. Kent-Braun JA, Miller RG, Weiner MW. Magnetic resonance spectroscopy studies of human muscle. *Radiol Clin North Am.* 1994; 32(2):313–335. [PubMed: 8140229]

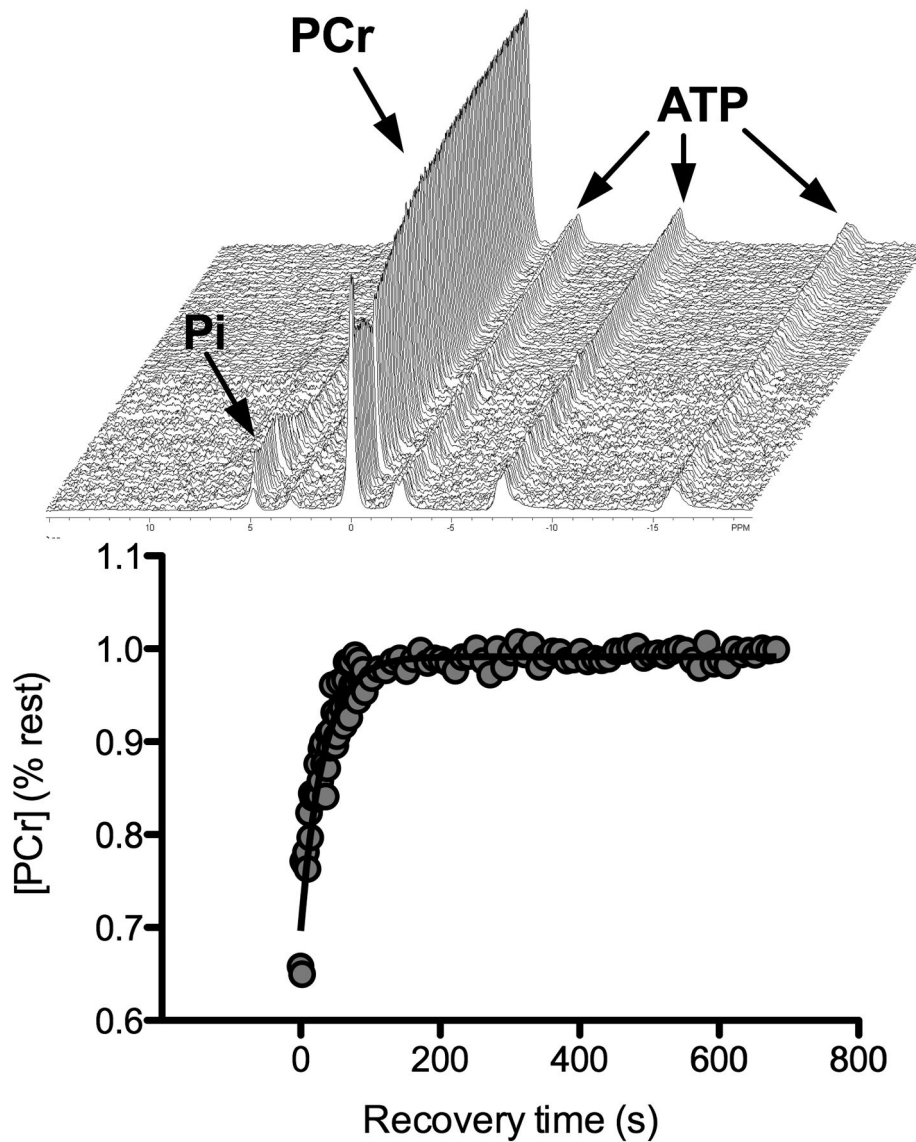


**Figure 1.  $^{31}\text{P}$  MRS spectra and PCr recovery in a single subject**  
 Representative stackplot of phosphorous spectra at rest (first spectrum, 60s average) and throughout the 30s muscle contraction (2s resolution) and 10 minute recovery (top panel). Monoexponential fit of PCr during the recovery period in the same individual is shown by the solid black line (bottom panel).

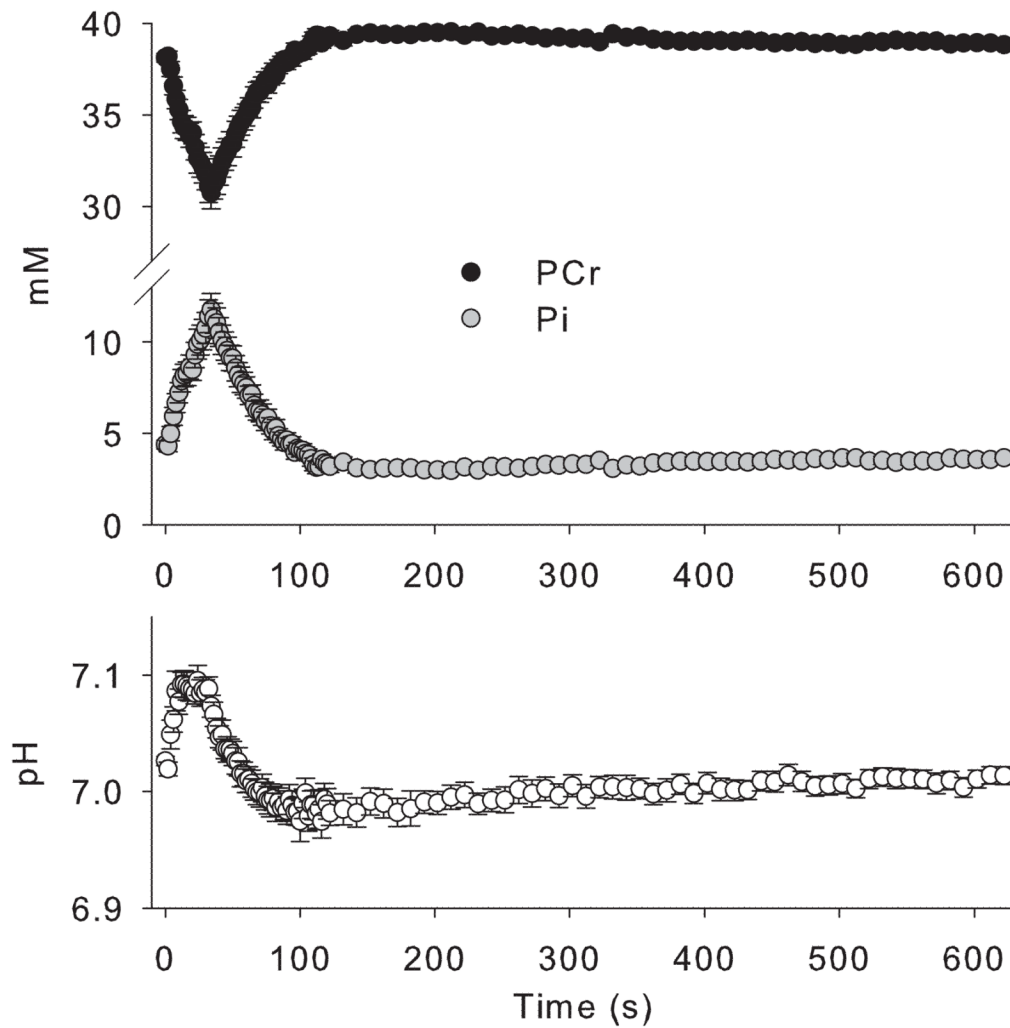


**Figure 2. Average PCr, Pi, and pH during rest, exercise and recovery**  
Phosphocreatine (black circles) transiently decreased during 30 seconds of exercise, while inorganic phosphate (grey circles) increased. Both metabolites recovered rapidly upon cessation of the muscle contraction. pH (white circles) exhibited the expected alkalosis during exercise and minimal acidosis during recovery. Data are mean  $\pm$  SEM.

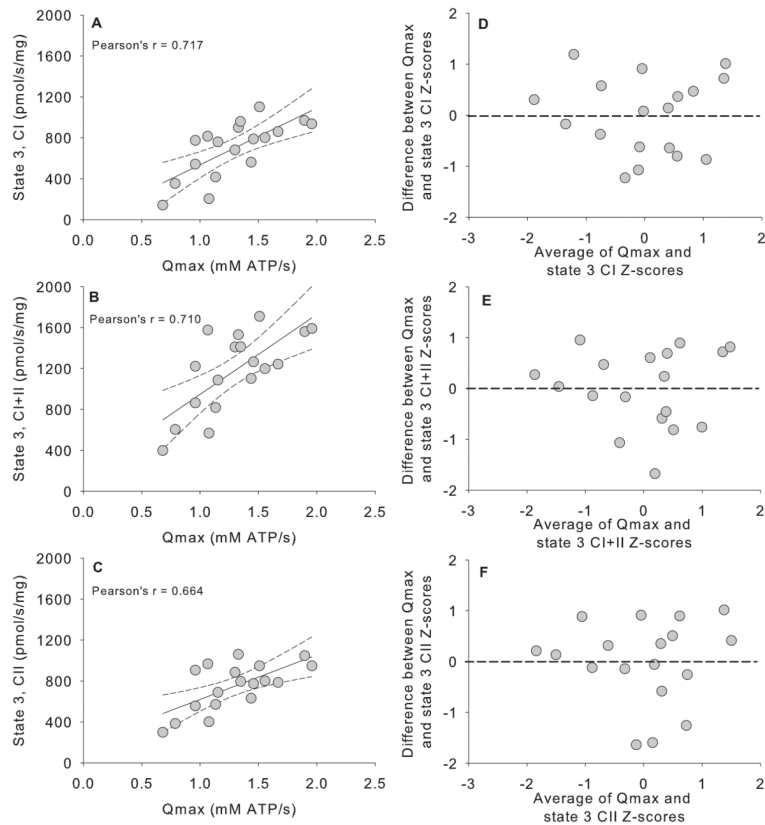


**Figure 3. Comparison of *in vitro* to *in vivo* indices of muscle oxidative capacity**

Panels A, B, and C show correlations between oxidative capacity measured by  $^{31}\text{P}$ -MRS ( $Q_{max}$ ) and maximal respiration in isolated mitochondria in the presence of substrates for respiratory chain complex I (state 3, CI, Panel A), complex I+II (state 3, CI+II, Panel B), and complex II (state 3, CII, Panel C). Pearson correlation coefficients are given for each relationship. Solid black lines represent linear regression between each variable with the 95% confidence intervals as dashed lines. Panels D, E, and F show the level of agreement between *in vitro* and *in vivo* measurements as Bland-Altman plots of z-scores calculated for  $Q_{max}$  vs. complex I (panel D),  $Q_{max}$  vs. complex I+II (panel E), and  $Q_{max}$  vs. complex II (panel F).

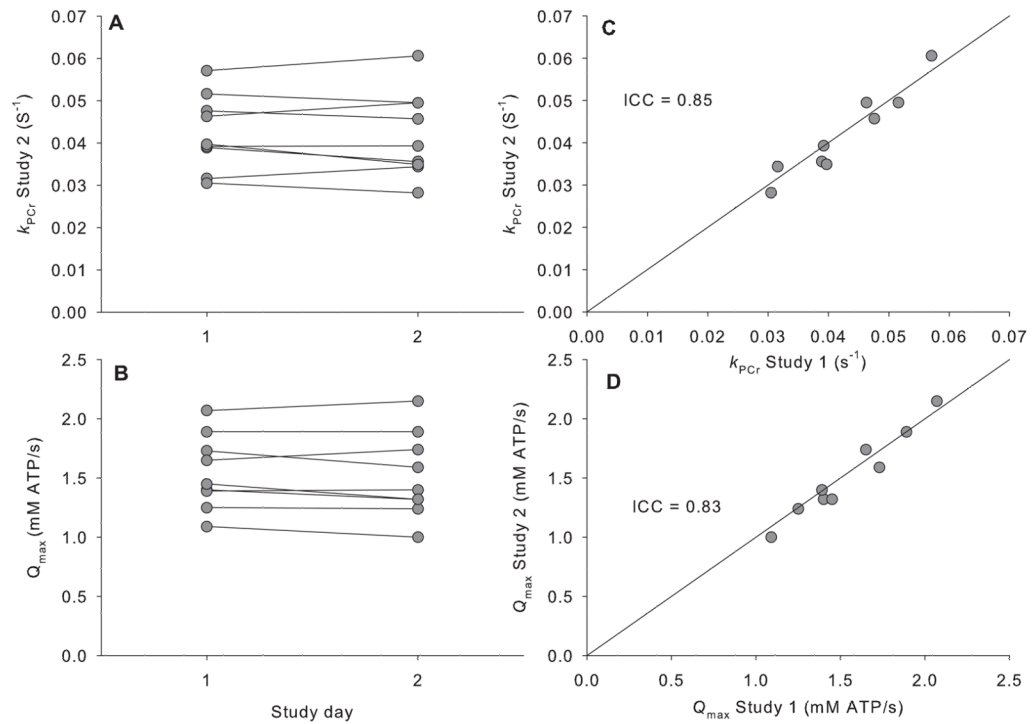


**Figure 4. Reproducibility of 31P-MRS for measuring oxidative capacity**

Individual values for the PCr recovery rate constants ( $K_{PCr}$ , panel A) and computed oxidative capacity ( $Q_{max}$ , panel B) measured on 2 different days. Panels C and D show correlations between  $K_{PCr}$  (C) and  $Q_{max}$  (D) for each study day with the solid black line representing the line of identity. Intra-class correlation coefficients (ICC) are given for each variable.

**Table 1****Metabolic Parameters**

Skeletal muscle mitochondrial respiration rates and respiratory control ratio (RCR) were measured in isolated mitochondria by high resolution respirometry. Phosphorous metabolites and pH at rest and end-exercise, and oxidative capacity were measured *in vivo* by  $^{31}\text{P}$ -MRS. Data are means  $\pm$  SEM.

<i>In vitro</i> parameters	
State 2 (pmol/s/mg wet weight)	36.1 $\pm$ 2.8
State 3, complex I (pmol/s/mg wet weight)	698.7 $\pm$ 64.2
State 3, complex I+II (pmol/s/mg wet weight)	1175.6 $\pm$ 91.4
State 3, complex II (pmol/s/mg wet weight)	747.5 $\pm$ 54.4
State 4 (pmol/s/mg wet weight)	165.2 $\pm$ 28.5
RCR	8.50 $\pm$ 0.75
<i>In vivo</i> parameters	
PCr <sub>rest</sub> (mM)	38.10 $\pm$ 0.24
Pi <sub>rest</sub> (mM)	4.39 $\pm$ 0.24
pH <sub>rest</sub>	7.03 $\pm$ 0.004
PCr <sub>ex</sub> (mM)	30.73 $\pm$ 0.88
Pi <sub>ex</sub> (mM)	11.77 $\pm$ 0.88
pH <sub>ex</sub>	7.07 $\pm$ 0.009
k <sub>PCr</sub> (s <sup>-1</sup> )	0.034 $\pm$ 0.002
Q <sub>max</sub> (mM ATP/s)	1.29 $\pm$ 0.08

**Table 2**  
**Metabolic parameters measured by  $^{31}\text{P}$ -MRS parameters**

Resting and end-exercise phosphorous metabolites, pH, PCr recovery rate constant ( $k_{\text{PCr}}$ ), oxidative capacity ( $Q_{\text{max}}$ ), and the force-time integral (FTI) measured in the same individuals on 2 days (N=9). Data are means  $\pm$  SEM

<i>In vivo</i> parameters	Test 1	Test 2	CV (%)	P (paired ttest)
PCr <sub>rest</sub> (mM)	36.56 $\pm$ 0.40	36.07 $\pm$ 0.39	2.21 $\pm$ 0.66	0.36
Pi <sub>rest</sub> (mM)	5.94 $\pm$ 0.40	6.43 $\pm$ 0.39	14.6 $\pm$ 5.3	0.36
pH <sub>rest</sub>	7.05 $\pm$ 0.006	7.04 $\pm$ 0.004	0.16 $\pm$ 0.03	0.79
PCr <sub>ex</sub> (mM)	30.98 $\pm$ 0.61	30.17 $\pm$ 0.90	4.13 $\pm$ 1.14	0.30
Pi <sub>ex</sub> (mM)	11.51 $\pm$ 0.61	12.32 $\pm$ 0.90	10.0 $\pm$ 2.8	0.30
pH <sub>ex</sub>	7.11 $\pm$ 0.02	7.12 $\pm$ 0.03	0.60 $\pm$ 0.22	0.91
$k_{\text{PCr}}$	0.042 $\pm$ 0.003	0.042 $\pm$ 0.003	4.65 $\pm$ 0.84	0.62
$Q_{\text{max}}$ (mM ATP/s)	1.55 $\pm$ 0.10	1.52 $\pm$ 0.12	3.37 $\pm$ 0.86	0.32
FTI (N·s)	6520 $\pm$ 392	6713 $\pm$ 380	7.81 $\pm$ 1.96	0.54